# Scaling relation between $pA$ and $AA$ collisions

Gökçe Başar* and Derek Teaney†
*Department of Physics and Astronomy, Stony Brook University, Stony Brook, New York 11794, USA*
(Received 4 March 2014; revised manuscript received 13 August 2014; published 6 November 2014)

We compare the flowlike correlations in high multiplicity proton-nucleus ($p + A$) and nucleus-nucleus ($A + A$) collisions. At fixed multiplicity, the correlations in these two colliding systems are strikingly similar, although the system size is smaller in $p + A$. Based on an independent cluster model and a simple conformal scaling argument, where the ratio of the mean free path to the system size stays constant at fixed multiplicity, we argue that flow in $p + A$ emerges as a collective response to the fluctuations in the position of clusters, just like in $A + A$ collisions. With several physically motivated and parameter free rescalings of the recent LHC data, we show that this simple model captures the essential physics of elliptic and triangular flow in $p + A$ collisions. We also explore the implications of the model for jet energy loss in $p + A$, and predict slightly larger transverse momentum broadening in $p + A$ than in $A + A$ at the same multiplicity.

DOI: 10.1103/PhysRevC.90.054903 PACS number(s): 24.10.Nz, 25.75.Nq

## I. INTRODUCTION

Recent measurements by the LHC [1–3] and RHIC [4] collaborations, have shown that particle production in high multiplicity proton-nucleus ($p + A$) collisions exhibits striking long-range two-particle correlations. Indeed, the two-particle correlator in these high multiplicity events is qualitatively and even quantitatively similar to the corresponding correlator in nucleus-nucleus ($A + A$) events. In the $A + A$ events the correlation function was successfully described with viscous hydrodynamics, where the observed correlation arises from the collective response to the initial geometry. The two-particle angular correlation at large rapidity separation is decomposed into Fourier coefficients,

$$\frac{dN_{\text{pairs}}}{d\Delta\phi} = \frac{N_{\text{pairs}}}{2\pi}\left[1 + 2\sum V_{n\Delta}\cos(n\Delta\phi)\right], \tag{1.1}$$

and the Fourier coefficients are expressed in terms of the flow coefficients $v_n\{2\}$,

$$v_n\{2\} \equiv \sqrt{V_{n\Delta}}. \tag{1.2}$$

The flow coefficients are measured as a function of momentum, particle type, and centrality and are compared to hydrodynamic simulations of the nucleus-nucleus event (see Ref. [5] for an overview of this ongoing experimental and theoretical program).

A comparison of the flow coefficients in peripheral $A + A$ to high multiplicity $p + A$ collisions, at the same overall multiplicity, shows that the flow coefficients are similar in magnitude and depend on momentum in similar ways. Indeed, the two collision systems have the same integrated $v_3\{2\}$ to within 5%. The striking similarity between the observed correlations points to a common origin, and challenges the hydrodynamic interpretation. Indeed, some features of these correlations are reproduced by the color glass condensate (CGC) without reference to the fluctuating geometry [6,7]. However, hydrodynamic simulations of $p + A$ events also qualitatively predicted the correlations observed in the data [8–10], suggesting that the origin of the flow in $p + A$ is similar to $A + A$. This has motivated several phenomenological papers aiming to explain the observed correlations and to differentiate these two approaches [11–18].

The purpose of the current paper is to give a concise explanation for the striking similarity of the flow harmonics in $p + A$ and $A + A$. We start by pointing out in Sec. II that if the multiplicity is held fixed, and the initial dynamics is approximately conformal, then the mean free path to system size is the same in the two colliding systems. The $p + A$ system is smaller than $A + A$, but hotter, and the resulting response patterns in $p + A$ are scale similar to the $A + A$ response. Thus, it is natural to expect that if a hydrodynamic response is supported in $A + A$ collisions then a similar response is expected in high multiplicity $p + A$ collisions. In $A + A$ collisions viscous corrections are somewhat large in these peripheral bins, and we expect similarly large corrections in $p + A$ collisions.

In Sec. III we discuss elliptic and triangular flow. After scaling out the average geometry of the $A + A$ system (which can be done in a model-independent way), we find that the integrated $v_2\{2\}$ in the two systems are essentially identical, as in the $v_3\{2\}$ case. We point out that this is not surprising in any picture based on an independent cluster model and approximately conformal dynamics. Because the process of scaling out the average geometry assumes that the observed $v_2\{2\}$ is a response to the geometry, the remarkable similarity of the fluctuation-driven $v_2\{2\}$ in the two systems strongly suggests that the response in the $p + A$ system is also a response to the geometry. The momentum dependence of the elliptic and triangular flow coefficients also supports the conformal scaling outlined in Sec. II.

Finally, in Sec. IV we discuss the implications of the conformal dynamics for jet energy loss in $p + A$, indicating a direction for future research.

*basar@tonic.physics.sunysb.edu
†derek.teaney@stonybrook.edu

 

## II. CONFORMAL DYNAMICS

### A. $\ell_{\rm mfp}/L$ is the constant in $p+A$ and $A+A$ collisions at fixed multiplicity

Working with a reasonable set of assumptions, we first note that the mean free path to system size is constant between high multiplicity $p+A$ and $A+A$ collisions, provided the multiplicity $dN/{\rm d}y$ is kept fixed.

Specifically, motivated by the color glass condensate [19], we will adopt the following model for particle production in high multiplicity $p+A$ and $A+A$ collisions.

(1) First, we will assume a cluster model, where the number of particles produced is proportional to the number of clusters. The typical momentum scale of the produced constituents in the initial state is set by the number of clusters per transverse area:

$$Q_s^2 \sim \frac{N_{\rm clust}}{\pi L^2}, \tag{2.1}$$

where $L$ is the transverse size of the high multiplicity events. We will assume that this is the only relevant momentum scale. A similar assumption was used in Ref. [14] to investigate the systematics of particle spectra in high multiplicity $p+A$ collisions.

(2) We will assume that the equilibration dynamics is conformal, so that the typical relaxation time $\tau_R$ is inversely proportional to $Q_s$. Then, if $Q_s L$ is a sufficiently large number, the system will equilibrate at a time $\tau_o$ with $1/Q_s \ll \tau_o \ll L$, and the initial temperature $T_{\rm o}$ will be proportional to $Q_s$, $T_{\rm o} \propto Q_s$. If the shear viscosity is approximately conformal, $\eta \propto T^3$, then viscous corrections from transverse gradients will be proportional to $1/(Q_s L)$.

Indeed, in kinetic theory transverse viscous corrections are determined by the ratio of the mean free path to the transverse size of the system. In conformal kinetics the initial mean free path is inversely proportional to $Q_s$, which is the only relevant momentum scale:

$$\ell_{\rm mfp} \propto \frac{1}{Q_s}. \tag{2.2}$$

(3) Finally, we will also assume that the initial phase space distribution in a high multiplicity $p+A$ event is not parametrically different from a minimum bias event. For instance, an extremely high multiplicity di-jet event has a parametrically different initial phase space distribution.

With these assumptions, the multiplicity of a $p+A$ or $A+A$ event is

$$\frac{dN}{dy} \sim Q_s^2 L^2. \tag{2.3}$$

Then mean free path to the transverse system size is constant, provided $dN/dy$ is kept fixed:

$$\frac{\ell_{\rm mfp}}{L} \propto \frac{1}{Q_s L} \propto \frac{1}{\sqrt{dN/dy}}. \tag{2.4}$$

This line of reasoning provides an extremely simple explanation for why the *collective* response is similar in high multiplicity $p+A$ and peripheral $A+A$ collisions. If the multiplicity is held fixed, then the conditions for the subsequent response in $p+A$ and $A+A$ are scale similar. The $p+A$ system is smaller, but hotter, and the initial temperature times the system size is fixed. If the subsequent expansion dynamics is approximately conformal, then the resulting collective response at a time, $\tau\, Q_s$, in the $p+A$ system will be equal to the $A+A$ response at the corresponding time. We will adopt this conformal scaling in what follows and investigate the attendant consequences.

The preceding estimate for $\ell_{\rm mfp}/L$ in Eq. (2.4) applies at the earliest moments while the system is expanding longitudinally. Specifically, we are considering times of order $\tau \sim \tau_o$ with $Q_s \ll \tau_o \ll L$. A more relevant time scale for the development of elliptic flow is $\tau \sim L$. To estimate the size of $\ell_{\rm mfp}/L$ for $\tau \sim L$, we recall the Bjorken result for the decrease in the initial temperature because of the longitudinal expansion [20],

$$T(\tau) = T_o \left(\frac{\tau_o}{\tau}\right)^{1/3}, \tag{2.5}$$

where $T_o$ and $\tau_o$ scale with the saturation momentum, $T_o \propto Q_s$ and $\tau_o \propto Q_s^{-1}$. Thus, at a time $\tau \sim L$ we have

$$\frac{\ell_{\rm mfp}}{L} \propto \frac{1}{T(\tau) L} \propto \frac{1}{(T_o L)^{2/3}} \propto \frac{1}{\sqrt[3]{dN/dy}}. \tag{2.6}$$

This estimate shows that for an approximately conformal fluid, viscous corrections to elliptic flow scale as $(dN/dy)^{-1/3}$, and are again independent of the transverse size provided the multiplicity is held fixed. This is consistent with the findings of more complete hydrodynamic simulations, where the conformal assumptions of this section are only approximately respected.

## III. ELLIPTIC AND TRIANGULAR FLOW

### A. Integrated flow coefficients

Because the mean free path to system size is the same in the two colliding systems, we expect that the integrated response $v_n/\epsilon_n$ should remain constant as one changes from $p+A$ to $A+A$ collisions.

We will adopt the independent cluster model to estimate $\epsilon_2\{2\}$ and $\epsilon_3\{2\}$ in $p+A$ and in $A+A$ [21]. Very recently, the independent cluster model was used (independently) to estimate the fluctuations in $\epsilon_n$ in $p+A$ events [12,18]. In $A+A$, the independent cluster model quantitatively reproduces the results of more sophisticated Glauber models [22]. In the independent cluster model, $N_{\rm clust}$ independent pointlike clusters are drawn from a smooth parent distribution, $\bar{n}(\boldsymbol{x})$. As discussed in the previous section, the multiplicity of an event is proportional to the number of the clusters, and the fluctuations in the cluster density in the transverse plane, $n(\boldsymbol{x}) = \bar{n}(\boldsymbol{x}) + \delta n(\boldsymbol{x})$, source the anisotropic collective flow. These fluctuations are assumed to be random such that

$$\langle \delta n(\boldsymbol{x}) \delta n(\boldsymbol{y}) \rangle = \bar{n}(\boldsymbol{x}) \delta^{(2)}(\boldsymbol{x}-\boldsymbol{y}). \tag{3.1}$$

The angular brackets denote an average over events with a fixed number clusters. We note that the current notation for the independent cluster model follows Ref. [23].

#### 1. Eccentricity and elliptic flow

The eccentricity is defined as

$$\epsilon_2 e^{i2\Phi_2} \equiv \frac{\{r^2 e^{i2\phi_s}\}}{\{r^2\}}, \tag{3.2}$$

where $\{\ldots\}$ denotes an average over the transverse plane in a single event. In $A+A$ collisions, there are two contributions to the eccentricity. The first contribution is the average ellipticity of the overlap region in noncentral collisions. This contribution is parametrized by the standard eccentricity $\epsilon_s$, which is the eccentricity of the smooth parent distribution. The second contribution comes from the fluctuations in the cluster density, which can be calculated using the statistics in Eq. (3.1). Using Eq. (12) of Ref. [21] [see also Eq. (15) of Ref. [23]], the mean squared eccentricity in $A+A$ collisions is

$$(\epsilon_2\{2\})^2_{AA} = \epsilon_s^2 + \langle\delta\epsilon_2^2\rangle + \mathcal{O}\left(\frac{\epsilon_s^2}{N_{\rm clust}}\right) + \mathcal{O}\left(\frac{1}{N^2_{\rm clust}}\right), \tag{3.3}$$

where fluctuation-driven eccentricity is

$$\langle\delta\epsilon_2^2\rangle = \frac{\langle r^4\rangle}{N_{\rm clust}\langle r^2\rangle^2}. \tag{3.4}$$

Here the averages are over the radial profile of the parent distribution, $\bar{n}(\boldsymbol{x})$. In $p+A$ collisions $\epsilon_s$ is presumably zero, and the squared eccentricity is determined only by fluctuations:

$$(\epsilon_2\{2\})^2_{pA} = \langle\delta\epsilon_2^2\rangle + \mathcal{O}\left(\frac{1}{N^2_{\rm clust}}\right). \tag{3.5}$$

The value of $\langle\delta\epsilon_2^2\rangle$ can differ in $p+A$ and $A+A$ collisions because the spatial distribution of clusters is not the same in the two systems. However, we do not expect this difference to be very important in determining $v_2\{2\}_{\rm pPb}/v_2\{2\}_{\rm PbPb}$ because the relevant parameter (at a fixed number of clusters) is the square root of a geometric double ratio,

$$\sqrt{\frac{\langle\delta\epsilon_2^2\rangle_{pA}}{\langle\delta\epsilon_2^2\rangle_{AA}}} = \sqrt{\frac{(\langle r^4\rangle/\langle r^2\rangle^2)_{pA}}{(\langle r^4\rangle/\langle r^2\rangle^2)_{AA}}}. \tag{3.6}$$

This parameter will always be close to unity for any reasonable shape. For example, comparing a hard sphere profile $\bar{n}(\boldsymbol{b}) \propto \sqrt{1-b^2/R_0^2}$ to a Gaussian, one finds

$$\sqrt{\frac{\langle\delta\epsilon_2^2\rangle_{\rm hard-sphere}}{\langle\delta\epsilon_2^2\rangle_{\rm Gaussian}}} \approx 0.85. \tag{3.7}$$

Thus, even with somewhat different profiles, the difference in the fluctuation-driven eccentricities $\sqrt{\langle\delta\epsilon_2^2\rangle}$ is only 15%. More importantly, demanding similar eccentricities to 5% accuracy does not require a fine tuning. Because a Gaussian profile for the $p+A$ event would arise in any diffusive process, this profile seems particularly important. In Fig. 1 we have computed the ratio in Eq. (3.6) for a Gaussian profile and the PHOBOS Glauber model as a function of $N_{\rm trk}^{\rm offline}$, and the result is unity to a few percent accuracy. The relation between $N_{\rm trk}^{\rm offline}$ and $N_{\rm part}$ is from Ref. [24].

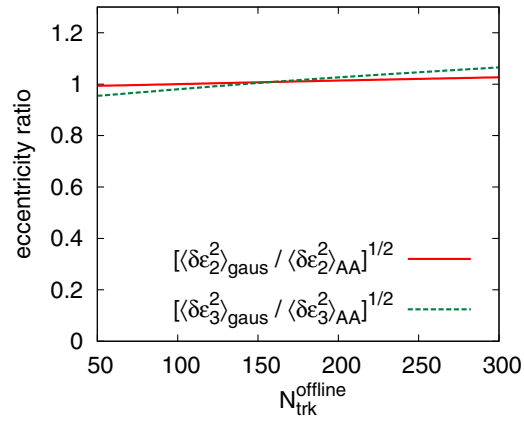


FIG. 1. (Color online) The ratio of fluctuation-driven eccentricities $\delta\epsilon_2$ and $\delta\epsilon_3$, for a Gaussian profile compared to the PHOBOS Glauber model [25] as a function of $N_{\rm trk}^{\rm offline}$. The precise definition of these quantities are given in Eqs. (3.6) and (3.12).

In the framework of linear response, elliptic flow is understood as a collective response to the eccentricity of the initial geometry such that $v_2 = k_2\epsilon_2$. The linear response coefficient $k_2$ depends only on the ratio of the mean free path to the system size. Therefore, the conformal scaling of Sec. II predicts that the $k_2$ coefficient is the same in $p+A$ and $A+A$ collisions at fixed multiplicity. To fairly compare the $v_2$ in $p+A$ and $A+A$ we should first remove dependence on the average geometry, and isolate the fluctuation-driven $v_2$ in $A+A$. This can be achieved by scaling the $v_2$ in $A+A$ by the appropriate factor $\sqrt{\epsilon_2\{2\}^2-\epsilon_s^2}/\epsilon_2\{2\}$, so that

$$\frac{\sqrt{\epsilon_2\{2\}^2-\epsilon_s^2}}{\epsilon_2\{2\}}(v_2\{2\})_{AA} = k_2\sqrt{\langle\delta\epsilon_2^2\rangle_{AA}}, \tag{3.8}$$

$$(v_2\{2\})_{pA} = k_2\sqrt{\langle\delta\epsilon_2^2\rangle_{pA}}. \tag{3.9}$$

It is useful to define a rescaled $v_2\{2\}$ for $A+A$ that isolates the fluctuations,

$$(v_2\{2\})_{\rm PbPb,rscl} \equiv \sqrt{1-\frac{\epsilon_s^2}{\epsilon_2\{2\}^2}}\,(v_2\{2\})_{\rm PbPb}. \tag{3.10}$$

We calculated the rescaling factor in Eq. (3.10) with the PHOBOS Glauber model [25] using the relation between $N_{\rm trk}^{\rm offline}$ and centrality provided by the CMS collaboration [24]. It should be stressed that this rescaling factor is a nontrivial function of impact parameter and multiplicity, and that there are no free parameters. This factor is completely determined by the Glauber model simulation of the $A+A$ event.

Similar rescalings have been used to explain the difference between $v_2\{2\}$ and $v_2\{4\}$ as a function of centrality in $A$+$A$ collisions [21,26]. Indeed, as in the current analysis, this difference primarily reflects the relative size of the average and fluctuating eccentricities [21].

In Fig. 2 we compare the fluctuation-driven part of the $(v_2\{2\})_{\rm PbPb}$ to $(v_2\{2\})_{\rm pPb}$. The data are taken from the CMS

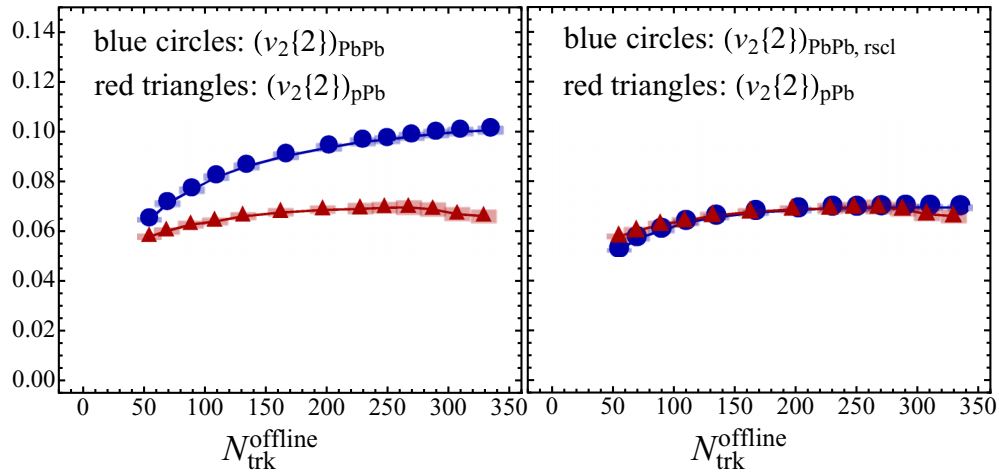


FIG. 2. (Color online) The integrated $v_2\{2\}$ for PbPb and pPb vs multiplicity from [24]. (Left) Original values. (Right) The fluctuation-dependent elliptic flow, $(v_2\{2\})_{\rm PbPb,rscl} = \sqrt{1-\epsilon_s^2/\epsilon_2\{2\}^2}\ (v_2\{2\})_{\rm PbPb}$, compared to $(v_2\{2\})_{\rm pPb}$. The scaling factor is extracted using the PHOBOS Glauber model [25] in $A+A$ simulations, and is not a fit.

collaboration [24]. The striking agreement between these curves after this geometric rescaling is a strong indication that the elliptic flow in $p+A$ stems from the same collective physics that determines the elliptic flow in $A+A$. As this rescaling was motivated by geometry, the response in the $p+A$ system should also be driven by the fluctuating geometry. Furthermore, the assumption that the two systems are related by a conformal rescaling, where the linear response coefficients are the same at fixed multiplicity, provides a concise explanation for the similar $v_2\{2\}$ in the two systems.

It is worth emphasizing that to calculate the eccentricity correction factor, $\sqrt{1-\epsilon_s^2/\epsilon_2\{2\}^2}$, we are using the $A+A$ Glauber model and not the $p+A$ Glauber model. There are significant uncertainties even in the $A+A$ Glauber model for these peripheral bins. However, these uncertainties correct a relatively modest correction factor, and are therefore small in Fig. 2. The uncertainty in $k_2 = v_2\{2\}/\epsilon_2\{2\}$ is larger (see Fig. 6 of Ref. [27]), but the precise value of $k_2$ is not needed for this analysis.

#### 2. *Triangularity and triangular flow*

Similar observations hold for $v_3\{2\}$. Because the triangularity is produced by the fluctuations in the cluster density and not the average geometry, the comparison is more direct. We define the triangularity,

$$\epsilon_3 e^{i3\Phi_3} \equiv \frac{\{r^3 e^{i3\phi_s}\}}{\{r^2\}^{3/2}}, \tag{3.11}$$

and compute the squared fluctuations of $\epsilon_3$ in $p+A$ and $A+A$ in the independent cluster model [22,23],

$$\langle\delta\epsilon_3^2\rangle = \frac{\langle r^6\rangle}{N_{\rm clust}\langle r^2\rangle^3}. \tag{3.12}$$

We have used an $r^3$ weight to define the triangularity. If an $r^2$ weight is used, all fluctuation-driven eccentricities are equal [23], i.e.,

$$\langle\delta\epsilon_2^2\rangle = \langle\delta\epsilon_3^2\rangle = \frac{\langle r^4\rangle}{N_{\rm clust}\langle r^2\rangle^2} \quad (r^2\ \text{weight}). \tag{3.13}$$

The optimal radial weight should be chosen to maximize the correlation between the flow response and the geometric predictor [28]. With either weight, the relevant parameter for determining the ratio of $v_3$ in the two colliding systems is

$$\sqrt{\frac{\langle\delta\epsilon_3^2\rangle_{pA}}{\langle\delta\epsilon_3^2\rangle_{AA}}}. \tag{3.14}$$

This will be close to unity for reasonable profiles, though the deviation from unity is potentially larger when the $r^3$ weight is used. For a Gaussian profile $p+A$ profile (which seems particularly well motivated), we compare $\langle\delta\epsilon_3^2\rangle_{\rm gaus}$ to the nuclear profile in Fig. 1 and the result is unity to within 5%.

Enforcing conformal dynamics on the linear response, we are led to the conclusion that the triangular flow in $p+A$ and $A+A$ collisions at a given multiplicity should be approximately the same,

$$(v_3\{2\})_{pA} = k_3\sqrt{\langle\delta\epsilon_3^2\rangle_{pA}}, \tag{3.15}$$

$$(v_3\{2\})_{AA} = k_3\sqrt{\langle\delta\epsilon_3^2\rangle_{AA}}. \tag{3.16}$$

Again, the linear response coefficient $k_3$ is constant at fixed multiplicity. In Fig. 3 we compare the CMS measurements of $v_3$ for pPb and PbPb collisions [24]. As in the elliptic case, the agreement between the $v_3$ measurements is remarkable. Empirically the ratio of triangular flows is $(v_3\{2\})_{\rm pPb}/(v_3\{2\})_{\rm PbPb} \approx 0.96$. The deviation from unity could be the result of corrections to the conformal scaling, or to the difference in the geometries of the colliding systems.

### B. Momentum dependence of the flow coefficients

Having provided a simple explanation for the integrated flow coefficients, which captures the essential physics, we

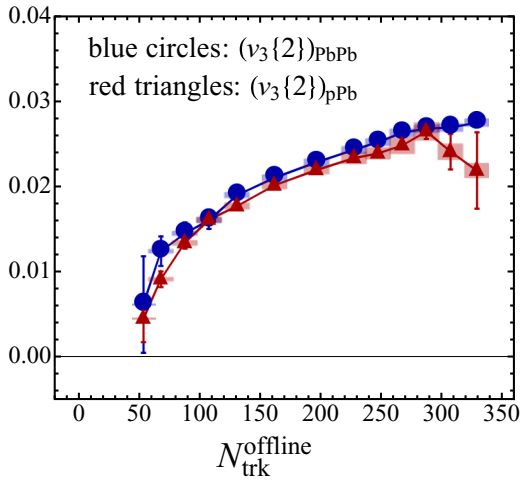


FIG. 3. (Color online) The integrated $v_3\{2\}$ for PbPb and pPb vs multiplicity from [24]. An approximately conformal response leads to $(v_3\{2\})_{\rm pPb} \simeq (v_3\{2\})_{\rm PbPb}$ at fixed multiplicity.

now study the momentum dependence. The conformal scaling that we discussed in Sec. II, suggests that each dimensionful observable can be written as the initial temperature $T_{\rm i} \propto Q_s$ to the appropriate power, times a dimensionless function of $T_{\rm i}L$. $T_{\rm i}L$ is constant at fixed multiplicity and is thus independent of the colliding system. In particular, we expect the mean transverse momentum at fixed multiplicity to be larger in $p+A$ than in $A+A$, because the $p+A$ system has a smaller transverse size. The expected increase in $p+A$ of the mean $\langle p_T\rangle$ and radial flow was also pointed out in [13], and was confirmed by the ALICE collaboration [29,30]. In addition, a dimensional analysis along these lines was recently used to analyze particle spectra in high multiplicity $p+A$ events [14].

In the small momentum regime $p_T \sim \langle p_T\rangle$, the flow coefficients grow linearly with momentum. Using the conformal scaling, we expect that

$$\frac{v_n}{\epsilon_n} = \xi_n \frac{p_T}{\langle p_T\rangle}, \tag{3.17}$$

where the dimensionless slopes $\xi_n$ depend only on the ratio of mean free path to system size, and are the same for $p+A$ and $A+A$ at fixed multiplicity. Starting from the observation that $\langle p_T\rangle$ in pPb is roughly 1.25 times higher than in PbPb [29,30], we will rescale the $p_T$ axes of the momentum dependent flow coefficients $(v_2\{2\}(p_T))_{\rm PbPb,rscl}$ and $(v_3\{2\}(p_T))_{\rm PbPb}$ with the factor,

$$\kappa \equiv \frac{\langle p_T\rangle_{\rm pPb}}{\langle p_T\rangle_{\rm PbPb}} \approx 1.25, \tag{3.18}$$

to compare the dimensionless slopes in the two colliding systems. Thus, for $v_2$ we expect the following scaling relation

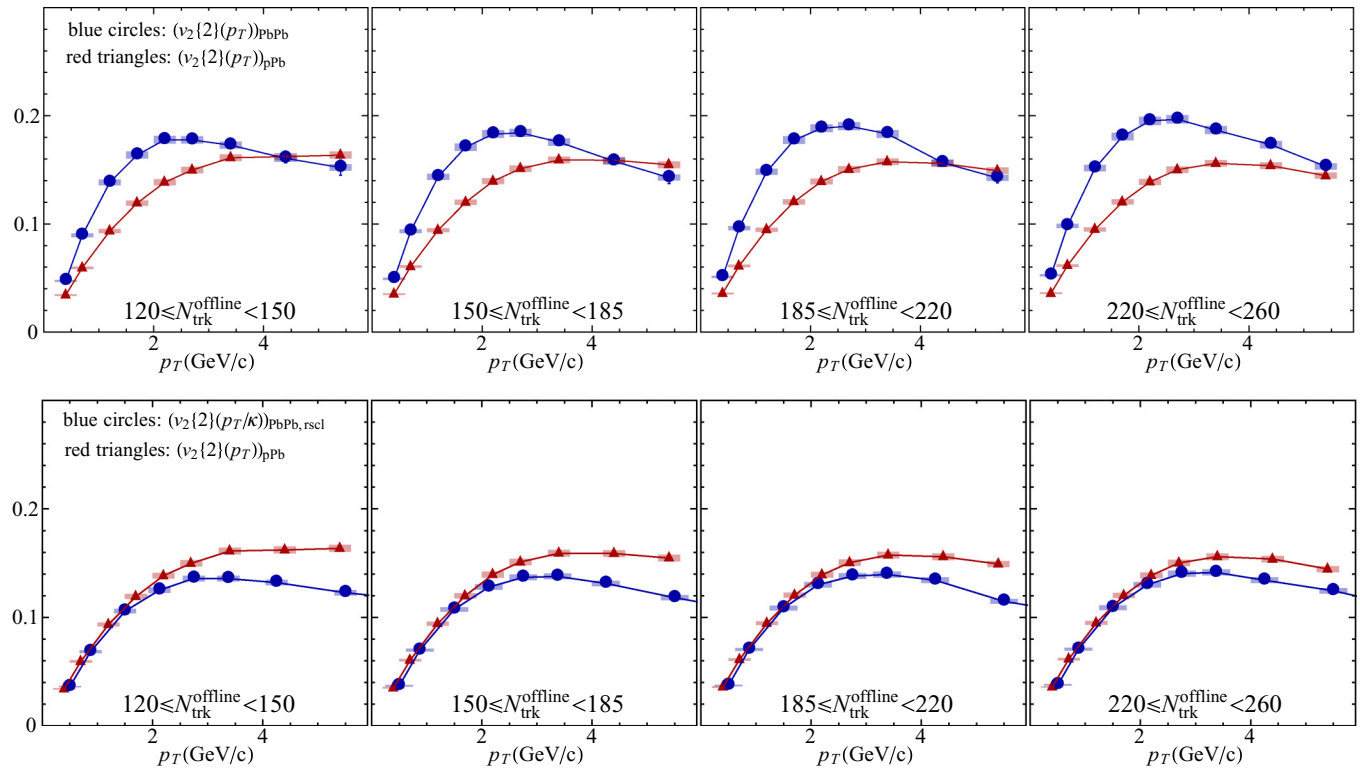


FIG. 4. (Color online) A comparison of the momentum dependent $v_2\{2\}$ in pPb and PbPb collisions. (Upper) Original data. (Lower) The PbPb data is rescaled to isolate the fluctuation-driven part of the elliptic flow as defined in Eq. (3.10). The momentum axis is also scaled by the conformal scaling factor $\kappa \approx 1.25$, Eq. (3.18). This is a parameter free rescaling. The agreement in the low $p_T$ region suggests that elliptic flow in $p+A$ results from a linear response to the fluctuations of the initial geometry which is conformally related to the $A+A$ response. The data are from Ref. [24].

between the pPb and PbPb systems:

$$(v_2\{2\}(p_T))_{\rm pPb} = \sqrt{1-\frac{\epsilon_s^2}{\epsilon_2\{2\}^2}}\,(v_2\{2\}\,(p_T/\kappa))_{\rm PbPb}\,. \quad (3.19)$$

The original data for $v_2$ and $v_3$ together with this complete (and parameter free) rescaling is shown in Figs. 4 and 5, respectively. From the lower panels in Figs. 4 and 5, we see that the agreement between the dimensionless slopes in the low $p_T$ region is remarkable, and seems to affirm the conformal rescaling. At higher $p_T$, the $v_2\{2\}$ start to systematically differ. This difference seems to become larger for lower multiplicities where nonflow could become significant.

An immediate consequence of the conformal scaling in Eq. (3.17) is that the breakdown of the linear regime, where the flow coefficients peak and start to decrease for larger $p_T$, should happen at a larger $p_T$ for $p+A$ compared to $A+A$. By comparing the pPb and PbPb measurements in the upper panels in Figs. 4 and 5 we can see that the maximum for both $v_2\{2\}$ and $v_3\{2\}$ is systematically at larger $p_T$ in pPb. Rescaling the $p_T$ axis by $\kappa$ as motivated by the conformal scaling brings these maxima into alignment.

It would be interesting to extend this analysis to different particle species. We are assuming that the fully inclusive $v_2(p_T)$ best reflects the conformal dynamics of the initial state. At freeze-out, the dynamics cannot be strictly conformal [31], and the presence of additional scales means that different particle species can receive different viscous corrections [32].

## IV. A QUALITATIVE ENERGY LOSS ANALYSIS FOR $p+A$

In this section we will qualitatively sketch the implications of the conformal scaling discussed in Sec. II for parton energy loss. For reviews of energy loss see [33–35]. A hard parton of energy $E$, traveling in the medium experiences energy loss from mainly two sources: collisions in the medium and medium induced radiation. The collisional energy loss can be parametrized by the drag coefficient $\hat{e}$, where $dE/dt = -\hat{e}$. To estimate the medium induced radiation, we will adopt the Baier-Dokshitzer-Mueller-Peigne-Schiff (BDMPS) framework [36,37], giving a heuristic review before discussing the implications for $p+A$ collisions [34].

The underlying physics can be understood as the interplay among the different scales in the problem: the formation length $\ell_{\rm form} \sim \omega/k_\perp^2$, the mean free path $\ell_{\rm mfp}$, and the system size $L$. The accumulation of transverse momentum squared $\langle k_\perp^2\rangle$ of the radiated gluons as the parton traverses the medium is modeled by a random walk in momentum space with diffusion coefficient $\hat{q}$, where $\hat{q} = d\langle k_\perp^2\rangle/dt$. The medium induced radiation spectrum has several regimes, depending on the frequency $\omega$ of the radiated gluon:

(i) In the Bethe-Heitler regime where $\omega < \hat{q}\,\ell_{\rm mfp}^2$ and $\ell_{\rm form} < \ell_{\rm mfp}$, the radiation spectrum is of order,

$$\omega\frac{dN_g}{d\omega\,{\rm d}z} \sim \frac{\alpha_{\rm s}}{\ell_{\rm mfp}} \quad \left(\omega < \hat{q}\,\ell_{\rm mfp}^2\right). \quad \text{(Bethe-Heitler)}$$

The radiation in this soft frequency range can be neglected in simulations of parton energy loss.

(ii) In the LPM regime where $\hat{q}\,\ell_{\rm mfp}^2 < \omega < \hat{q}\,L^2$ and $\ell_{\rm mfp} < \ell_{\rm form} < L$, the radiation is depleted by destructive interference between several subsequent scatterings. Effectively $N = \ell_{\rm form}/\ell_{\rm mfp}$ scatterings act like one scattering center for the induced radiation. This is the Landau-Pomeranchuk-Migdal (LPM) effect, and the formation time in this regime should be calculated self-consistently to take into account the destructive interference. Because the average $k_\perp^2$ after $N$ collisions is $\hat{q}\,\ell_{\rm form}$, we obtain the relation $\ell_{\rm form} \sim \omega/\hat{q}\,\ell_{\rm form}$. Thus, the gluon spectrum in the LPM regime is of order,

$$\omega\frac{dN_g}{d\omega\,{\rm d}z} \sim \frac{\alpha_{\rm s}}{\ell_{\rm mfp}}\frac{1}{N} \sim \alpha_{\rm s}\sqrt{\frac{\hat{q}}{\omega}} \quad \left(\text{with} \quad \hat{q}\,\ell_{\rm mfp}^2 < \omega < \hat{q}\,L^2\right). \quad \text{(LPM)}$$

(iii) Finally in the deep LPM regime where $\omega > \hat{q}\,L^2$, the formation length of the radiation exceeds the size of the medium $\ell_{\rm form} > L$, and the medium acts as a single scattering center. In this regime the medium induced radiation spectrum is of order,

$$\omega\frac{d(\Delta N_g)}{d\omega} \sim \alpha_{\rm s}\left(\frac{L}{\ell_{\rm form}}\right)^2 \sim \alpha_{\rm s}\frac{(\hat{q}L^2)^2}{\omega^2} \quad (\text{with} \quad \omega > \hat{q}\,L^2), \quad \text{(deep-LPM)}$$

where $\Delta N_g = N_g - N_g^{\rm vac}$ is the number of gluons emitted in excess of the vacuum shower.

The relation between the average energy loss $\Delta E$ and the system size depends on the initial energy of the parton. For example, for $E < \hat{q}\,L^2$ the parton never experiences the deep LPM regime. In this case, the average energy loss is found by integrating the appropriate radiation spectrum (LPM) over the path length and frequency from $\omega = 0\ldots E$:

$$\Delta E \sim \alpha_{\rm s}\sqrt{E\hat{q}}\,L \quad (\text{for } E < \hat{q}\,L^2). \quad (4.1)$$

A more energetic parton, with $E > \hat{q}\,L^2$, experiences the deep LPM suppression, and integrating the corresponding radiation spectrum (deep-LPM) from $\omega = \hat{q}L^2\ldots\infty$ yields [34,36,37]

$$\Delta E \sim \alpha_{\rm s}\,\hat{q}L^2 \quad (\text{for } E > \hat{q}\,L^2). \quad (4.2)$$

We can now discuss the implications of the conformal scaling framework for jet energy loss. Let us denote the critical energy that separates these two regimes as $E_{\rm cr} = \hat{q}\,L^2$. The conformal scaling from $A+A$ to $p+A$ predicts that $E_{{\rm cr},pA} = \hat{q}_{pA}\,L_{pA}^2 = \kappa\,\hat{q}_{AA}\,L_{AA}^2$ where $\kappa = L_{AA}/L_{pA}$ is the scaling factor. This scaling of $E_{cr}$ from $p+A$ to $A+A$ follows from $\hat{q} \sim T^3$ and the prediction of the conformal dynamics where $T_{pA} = \kappa T_{AA}$. Because $E_{{\rm cr},pA} > E_{{\rm cr},AA}$, the deep LPM regime (which is associated with *small* systems) is achieved *later* as a function of increasing total parton energy $E$ for the $p+A$ collisions. This counterintuitive result occurs because, in addition to the decrease in the system size, the conformal scaling leads to an increase in $\hat{q}$. The increase in $\hat{q}$ translates into a decrease in the typical formation length, requiring more energy to reach the transitional point where the formation length exceeds the system size. The same

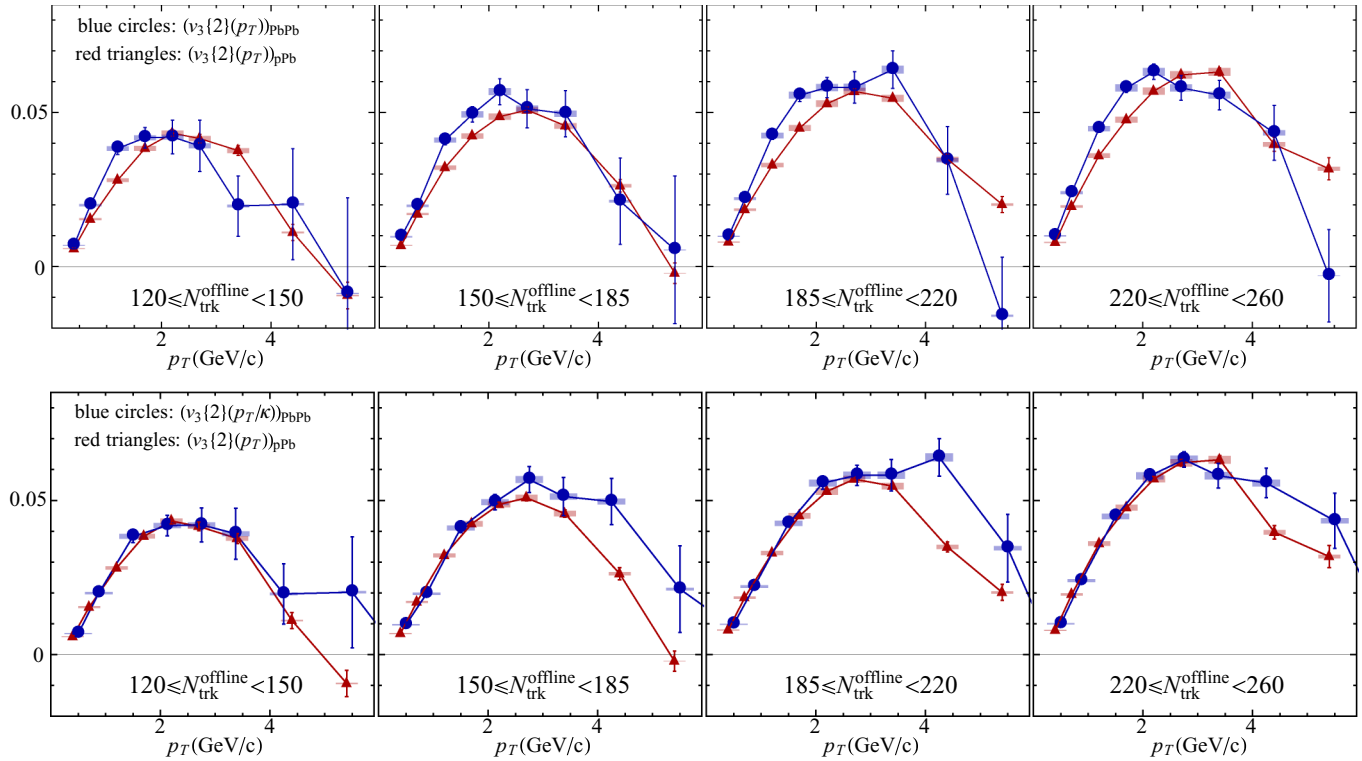


FIG. 5. (Color online) The comparison of the momentum-dependent $v_3\{2\}$ in pPb and PbPb collisions. (Upper) Original data. (Lower) The momentum axis is scaled by the conformal scaling factor $\kappa \approx 1.25$, Eq. (3.18). This is a parameter free rescaling. The agreement in the low $p_T$ region suggests that the triangular flow in $p + A$ results from a linear response to the fluctuations in the initial geometry which is conformally related to the $A + A$ response. The data are from Ref. [24].

reasoning also predicts somewhat larger transverse momentum broadening for jets produced in $p + A$ collisions.

A more quantitative analysis of jet energy loss in $p + A$ is left for future work. We hope that qualitative (and counterintuitive) features of the conformal scaling outlined in this section can survive in a more complete treatment of parton energy loss.

## V. SUMMARY AND DISCUSSION

By analyzing the flow measurements of pPb and PbPb collisions at the LHC with several physically motivated rescalings, we provide evidence for a collective response to the geometry in high multiplicity pPb collisions.

First, we note that once the average ellipticity is scaled out of the PbPb elliptic flow, the fluctuation-driven integrated $v_2\{2\}$ in PbPb is the same as in pPb at fixed multiplicity (Fig. 2). The integrated triangular flows in these two colliding systems are already equal. It seems to us phenomenologically untenable to ascribe different physics to the $p + A$ and $A + A$ flow measurements. Because the rescaling in PbPb was entirely motivated by linear response and geometry, we conclude that both the elliptic and triangular flow in pPb should also be understood as a linear response to initial geometric fluctuations. Sections II and III A 1 offer a direct explanation for why the response coefficients and fluctuation-driven eccentricities in these two systems are similar at fixed multiplicity.

First, a simple estimate based on approximate conformal symmetry at high energies shows that the mean free path to system size in the two systems is constant at fixed multiplicity (see Sec. II). Thus, the dynamical response of the $p + A$ and $A + A$ systems are related by a simple conformal rescaling of the initial temperature and the system size such that $\ell_{\rm mfp}/L \propto 1/(T_{\rm i}L) =$ constant. The pPb system is smaller, but also hotter, leading to the same response at fixed multiplicity.

Next we used the independent cluster model to estimate the eccentricities in both systems. (In PbPb the independent cluster model reproduces the results of more sophisticated Glauber models [22].) Assuming that the multiplicity is proportional to the number of clusters, we find that the ratio of fluctuation-driven eccentricities in the two colliding systems is determined by a square root of a geometric double ratio, e.g.,

$$\sqrt{\frac{\langle\delta\epsilon_2^2\rangle_{pA}}{\langle\delta\epsilon_2^2\rangle_{AA}}} = \sqrt{\frac{(\langle r^4\rangle/\langle r^2\rangle^2)_{pA}}{(\langle r^4\rangle/\langle r^2\rangle^2)_{AA}}}. \tag{5.1}$$

The importance of this and related formulas is that even quite different $p + A$ profiles lead to approximately the same $\sqrt{\langle\delta\epsilon_2^2\rangle}$ and $\sqrt{\langle\delta\epsilon_3^2\rangle}$. Without fine tuning the profile it is reasonable to expect that the fluctuation-driven eccentricities in the two systems are equal to $\sim$5% accuracy. For a Gaussian $p + A$ profile, which arises in any diffusive process and seems particularly apropos, this double ratio is shown in Fig. 1 and is close to unity for both the second and third eccentricities.

The $p_T$ dependence of the elliptic and triangular flow gives additional evidence supporting the conformal scaling described above. The $\langle p_T \rangle$ and the slope of both $v_2\{2\}(p_T)$, $v_3\{2\}(p_T)$ scale in the same way between pPb and PbPb as expected from the conformal scaling of Sec. II. Indeed, the rescalings in Figs. 4 and 5 are essentially parameter free, given the measured $\langle p_T \rangle$ in both colliding systems. The agreement between the dimensionless slopes in the low $p_T$ region in these figures corroborates the conformal scaling outlined in Sec. II.

Finally, we have outlined several qualitative expectations of conformal scaling for energy loss. In particular, the finite size transition in energy loss, from a linear ($\Delta E \propto L$) to a quadratic ($\Delta E \propto L^2$) length dependence, requires *higher* energy for the initial parton in the $p + A$ system. While a quantitative discussion and simulation of energy loss is left for future work, the conformal scaling arguments of Sec. IV suggest that the energy loss and transverse momentum broadening of jets should be somewhat larger in $p + A$ than in $A + A$ at the same multiplicity. Because the energy loss in $A + A$ is fairly mild in these peripheral bins,[1] and because preliminary measurements of jet energy loss in $p + A$ are at somewhat low multiplicity [39], this prediction does not seem in contradiction with current measurements, which do not indicate energy loss.

In summary, we have provided a concise explanation for why the angular correlations in pPb and PbPb collisions are similar—these correlations are the result of an approximately conformal response to fluctuation-driven eccentricities. It is important to emphasize that any conformal response to the geometry will yield similar correlations in the two colliding systems. However, it is equally important to emphasize that any conformal dynamics will asymptote to conformal hydrodynamics in the limit of high multiplicity.

[1] See, for example, the 50%–60% centrality bin in Fig. 6 of Ref. [38].

## ACKNOWLEDGMENTS

We thank A. Bzdak, D. Kharzeev, R. Venugopalan, E. Shuryak, L. Yan, Y. Yin, and I. Zahed for useful discussions. We also thank J.-Y. Ollitrault, U. Heinz, and T. Schaefer for a discussion of the $dN/dy$ scaling of viscous corrections. This work was supported by the U.S. Department of Energy under Grants No. DE-FG-88ER40388 (G.B.) and No. DE-FG-02-08ER4154 (D.T.).

[1] Serguei Chatrchyan *et al.* (CMS Collaboration), Phys. Lett. B **718**, 795 (2013).
[2] Georges Aad *et al.* (ATLAS Collaboration), Phys. Rev. Lett. **110**, 182302 (2013).
[3] Betty Abelev *et al.* (ALICE Collaboration), Phys. Lett. B **719**, 29 (2013).
[4] A. Adare *et al.* (PHENIX Collaboration), Phys. Rev. Lett. **111**, 212301 (2013).
[5] Ulrich W Heinz and Raimond Snellings, Annu. Rev. Nucl. Part. Sci. **63**, 123 (2013).
[6] Kevin Dusling and Raju Venugopalan, Phys. Rev. D **87**, 051502 (2013).
[7] Kevin Dusling and Raju Venugopalan, Phys. Rev. D **87**, 094034 (2013).
[8] Piotr Bozek, Phys. Rev. C **85**, 014911 (2012).
[9] Piotr Bozek and Wojciech Broniowski, Phys. Lett. B **718**, 1557 (2013).
[10] Adam Bzdak, Bjoern Schenke, Prithwish Tribedy, and Raju Venugopalan, Phys. Rev. C **87**, 064906 (2013).
[11] Piotr Bozek, Adam Bzdak, and Vladimir Skokov, arXiv:1309.7358.
[12] Adam Bzdak, Piotr Bozek, and Larry McLerran, arXiv:1311.7325.
[13] Edward Shuryak and Ismail Zahed, Phys. Rev. C **88**, 044915 (2013).
[14] Larry McLerran, Michal Praszalowicz, and Bjoern Schenke, Nucl. Phys. A **916**, 210 (2013).
[15] Christopher E Coleman-Smith and Berndt Muller, Phys. Rev. D **89**, 025019 (2014).
[16] James D. Bjorken, Stanley J. Brodsky, and Alfred Scharff Goldhaber, Phys. Lett. B **726**, 344 (2013).
[17] Adrian Dumitru, Tuomas Lappi, and Larry McLerran, Nucl. Phys. A **922**, 140 (2014).
[18] Li Yan and Jean-Yves Ollitrault, Phys. Rev. Lett. **112**, 082301 (2014).
[19] See, for example, Francois Gelis, Edmond Iancu, Jamal Jalilian-Marian, and Raju Venugopalan, Ann. Rev. Nucl. Part. Sci. **60**, 463 (2010).
[20] J. D. Bjorken, Phys. Rev. D **27**, 140 (1983).
[21] Rajeev S. Bhalerao and Jean-Yves Ollitrault, Phys. Lett. B **641**, 260 (2006).
[22] Rajeev S. Bhalerao, Matthew Luzum, and Jean-Yves Ollitrault, Phys. Rev. C **84**, 054901 (2011).
[23] Jiangyong Jia and Derek Teaney, Eur. Phys. J. C **73**, 2558 (2013).
[24] Serguei Chatrchyan *et al.* (CMS Collaboration), Phys. Lett. B **724**, 213 (2013).
[25] B. Alver, M. Baker, C. Loizides, and P. Steinberg, arXiv:0805.4411.
[26] Georges Aad *et al.* (ATLAS Collaboration), JHEP **11**, 183 (2013).
[27] B. Alver, B. B. Back, M. D. Baker, M. Ballintijn, D. S. Barton *et al.*, Phys. Rev. C **77**, 014906 (2008).
[28] Fernando G. Gardim, Frederique Grassi, Matthew Luzum, and Jean-Yves Ollitrault, Phys. Rev. C **85**, 024908 (2012).
[29] Betty Bezverkhny Abelev *et al.* (ALICE Collaboration), Phys. Lett. B **727**, 371 (2013).
[30] Betty Bezverkhny Abelev *et al.* (ALICE Collaboration), Phys. Lett. B **728**, 25 (2014).
[31] H. Niemi and G. S. Denicol, arXiv:1404.7327.
[32] Kevin Dusling, Guy D. Moore, and Derek Teaney, Phys. Rev. C **81**, 034907 (2010).
[33] R. Baier, D. Schiff, and B. G. Zakharov, Ann. Rev. Nucl. Part. Sci. **50**, 37 (2000).

[34] A very useful guideto the current discussion and relevant literature is Peter Brockway Arnold, Phys. Rev. D **80**, 025004 (2009).
[35] A. Majumder and M. Van Leeuwen, Prog. Part. Nucl. Phys. **66**, 41 (2011).
[36] R. Baier, Yuri L. Dokshitzer, Alfred H. Mueller, S. Peigne, and D. Schiff, Nucl. Phys. B **484**, 265 (1997).
[37] R. Baier, Yuri L. Dokshitzer, Alfred H. Mueller, S. Peigne, and D. Schiff, Nucl. Phys. B **483**, 291 (1997).
[38] Georges Aad *et al.* (ATLAS Collaboration), Phys. Lett. B **719**, 220 (2013).
[39] CMS Collaboration (CMS Collaboration), CMS-PAS-HIN-14-001, 2014.